PNAS RESEARCH ARTICLE | IMMUNOLOGY AND INFLAMMATION

Homeostatic, repertoire and transcriptional relationships between colon T regulatory cell subsets

Deepshika Ramanan[a,1], Kaitavjeet Chowdhary[a], Serge M. Candéias[b], Martina Sassone-Corsi[a], Adelaide Gelineau[a], Diane Mathis[a], and Christophe Benoist[a,2]

Contributed by Christophe Benoist; received July 7, 2023; accepted October 26, 2023; reviewed by David Artis and Tadatsugu Taniguchi

Foxp3$^+$ regulatory T cells (Tregs) in the colon are key to promoting peaceful coexistence with symbiotic microbes. Differentiated in either thymic or peripheral locations, and modulated by microbes and other cellular influencers, colonic Treg subsets have been identified through key transcription factors (TFs; Helios, Rorγ, Gata3, and cMaf), but their interrelationships are unclear. Applying a multimodal array of immunologic, genomic, and microbiological assays, we find more overlap than expected between populations. The key TFs (Rorγ, Helios, Gata3, and cMaf) play different roles, some essential for subset identity, others driving functional gene signatures. Functional divergence was clearest under challenge. Single-cell genomics revealed a spectrum of phenotypes between the Helios+ and Rorγ+ poles, different Treg-inducing bacteria inducing the same Treg phenotypes to varying degrees, not distinct populations. TCR repertoires in monocolonized mice revealed that Helios+ and Rorγ+ Tregs are related and cannot be uniquely equated to tTreg and pTreg. Comparison of spleen and colon repertoires revealed that 2 to 5% of clonotypes are shared between the locations. We propose that rather than the origin of their differentiation, tissue-specific cues dictate the spectrum of colonic Treg phenotypes.

TCR | peripheral differentiation | host/microbe

Significance

Intestinal Treg lymphocytes, which respond to microbial or food stimuli, are important in controlling the peaceful coexistence with symbiotic microbes at the boundary. Several phenotypes of intestinal Tregs have been described, with different transcriptional programs, origins of differentiation, and functional attributes. Using a broad panel of monocolonized and of knockout mice with deficiencies in key transcription factors, we show that these Treg subsets are more interconnected than previously thought, with common homeostatic niches and sharing of TCR clonotypes that implies a common origin. These observations have important implications in understanding the host/microbe interface and therapeutic implications given the role of these Treg subsets in inflammatory diseases and tumor progression.

The immune system in the digestive tract is exposed to a complex array of food antigens and microbes that provide essential support. Peaceful coexistence is essential, avoiding breach by microorganisms but also overexuberant immune responses to their products that intrinsically tend to activate innate immune receptors. In addition to physical barriers (mucus layers and epithelial tight junctions), a state of "active tolerance" involves immunoregulatory circuits, among which are FoxP3$^+$ T regulatory cells (Tregs). Tregs regulate mucosal immunity to both symbionts and pathobionts, acting on many types of immunocytes via anti-inflammatory cytokines and small molecule mediators, and help preserve intestinal physiology by promoting epithelial barrier functions and tissue repair (1–3).

Several subsets of intestinal Tregs have been described, characterized by their sensitivity to microbial influences, and by a particular transcription factor (TF), particularly Gata3, Helios, Rorγ, and cMaf (reviewed in ref. 3). Schematically, Gata3$^+$ Tregs mostly overlap with Helios$^+$ Tregs, while cMaf$^+$ Tregs largely overlap with Rorγ$^+$ Tregs (4–7). For the latter, whether Rorγ or cMaf is the key TF driver is unclear (6–9). Rorγ$^+$cMaf$^+$ Tregs, but not Helios$^+$Gata3$^+$ Tregs, are strongly tuned by gut bacteria, rare in germfree or antibiotic-treated mice, but induced by a number of individual microbes belonging to different families (6–10). Helios$^+$ Tregs are more abundant in the small intestine, while Rorγ$^+$ Tregs dominate in the colon, plausibly tied to differences in microbial load in these locations. In addition, a sizeable population of Rorγ$^-$Nrp1$^-$ Tregs in the small intestine is modulated by dietary antigens (11). Importantly, activity of FoxP3, the key identifying TF for Treg cells, appears somewhat dispensable in Rorγ$^+$ Tregs, while it is essential in Helios$^+$ Treg cells (12, 13).

Treg cells can differentiate in the thymus, or in peripheral locations. It is often stated that Helios$^+$Nrp1$^+$ Tregs are "tTregs" that differentiated in the thymus, while Rorγ$^+$ Tregs and related subsets are "pTregs" that derived from Tconv (conventional T) cells, under particular conditions of activation (7, 12, 14–16), but it is unclear whether this correspondence is absolute (3).

Microbe-dependent Rorγ$^+$ Tregs are thought to mediate tolerance to commensal and pathogenic bacteria. Rorγ$^+$cMaf$^+$ Tregs have been reported to dampen production of IFNγ, IL4, or IL17 by Teff (effector T) cells (7–9, 17), although different studies report different outcomes, perhaps resulting from variable microbial environments. Several studies suggest that deficiency in Rorγ$^+$cMaf$^+$ Tregs leads to more severe colitis (6–9, 12, 15, 18), intestinal mastocytosis, enhanced type 2 immune responses (12, 19), and susceptibility to food allergy (20). Seemingly contradictory effects of Rorγ$^+$ Tregs on IgA production and coating of bacteria have been reported (6, 17, 21, 22). Noxious effects of Rorγ$^+$ Tregs are also

Author contributions: D.R., K.C., and C.B. designed research; D.R., K.C., S.M.C., M.S.-C., and A.G. performed research; D.R. and K.C. analyzed data; K.C. and S.M.C. edited paper; D.M. and C.B. edited paper Supervised; and D.R., D.M., and C.B. wrote the paper.

Reviewers: D.A., Weill Cornell Medicine; and T.T., Tokyo Daigaku Kikin.

The authors declare no competing interest.

[1]Present address: NOMIS Center for Immunobiology and Microbial Pathogenesis, Salk Institute for Biological Studies, San Diego, CA 92037.

[2]To whom correspondence may be addressed. Email: cbdm@hms.harvard.edu.

This article contains supporting information online at https://www.pnas.org/lookup/suppl/doi:10.1073/pnas.2311566120/-/DCSupplemental.

Published December 8, 2023.

encountered in oncology: Their frequency increases in colorectal cancer, and they paradoxically promote IL17-mediated intestinal inflammation (23, 24). Helios$^+$Gata3$^+$ Tregs are thought to promote tissue repair, in good part because of their preferential expression of tissue repair transcripts (in particular *Areg*) (4, 5, 25). But Helios$^+$Gata3$^+$ Tregs also affect colitis in the T cell transfer model (5) and enteric graft-vs-host disease (26, 27). Helios$^+$Gata3$^+$ Tregs may also improve the outcome of colorectal cancer by suppressing Th17 responses and preventing excessive intestinal tissue damage (28). While these different roles have been proposed, there have not been comparative studies of Treg subset functions.

The relative proportions of intestinal Treg subsets are tuned by a number of external influences. Several other cell types influence intestinal Treg differentiation and homeostasis: CD103$^+$ dendritic cells (DCs), CX3CR1$^+$ macrophages, innate lymphoid cells (ILC) 3, eosinophils (1, 3, 3), and recently described populations of MHC-II$^+$ Rorγ$^+$ stromal/myeloid cells (29–31). The nervous system also influences the balance of intestinal Treg subsets (32, 33), involving substance-P and neuron-produced IL6 (32, 34), in a triangular cross talk between gut microbiota, enteric or extrinsic neurons, and Tregs. The balance of intestinal Treg populations is under genetic control (17), with an intriguing maternal transmission of the set-point of Rorγ$^+$ Tregs that can carry across generations.

An integrated perspective on the identity and homeostatic regulation of intestinal Tregs is still lacking, as we have only a limited grasp of their population dynamics and interrelationships. Do the different Treg subsets regulate each other, do they compete for the same homeostatic niches? How related and interconnected are they when compared by gene expression programs or by their TCR repertoires, and are their functions as distinct as previously reported? Further, it is unknown whether individual Rorγ$^+$ Treg-inducing microbes elicit solely quantitative variations or phenotypically different populations. For an integrative perspective, we analyzed panels of mice monocolonized with different Treg-inducing microbes or carrying conditional knockouts of the four main driving TFs. Single-cell parsing by RNAseq and ATACseq, complemented with TCR repertoire analysis of unprecedented depth, showed that the main Treg subsets are more interconnected than previously thought and that the simple models that equate phenotype with differentiation origin require reconsideration.

Results

Intestinal Treg Subsets Regulate Each Other to Maintain a Homeostatic Balance. A variety of phenotypes are found among intestinal Treg cells, but their homeostatic relationships are unclear. As a means of introduction, and consistent with previous reports, the flow cytometry plots of colonic Treg cells of Fig. 1*A* lay out the major groups of intestinal Treg cells: Helios$^+$ and Rorγ$^+$ Tregs appear the most mutually exclusive, cMaf$^+$ Tregs overlap mostly with Rorγ$^+$ Tregs, but some cMaf expression is also present in Rorγ-negative cells and is detectable in Helios$^+$ Tregs. Gata3 is expressed mostly by Helios$^+$ Tregs, but again not exclusively. About 20% of colonic Tregs are Rorγ-Helios- (hereafter double-negative, DN), only a minority of which express Gata3. FoxP3, the defining TF of Treg cells, was expressed largely identically in all subsets, perhaps slightly more in Helios$^+$ Tregs (Fig. 1*B*; some Rorγ-Helios- are also discernible, but these are highly variable and will not be dealt with further). Colonic Rorγ$^+$ Tregs appeared around weaning age (8, 35, 36). At postnatal day 5, almost all colonic Tregs were Helios$^+$, DN Tregs expanding a week later, possibly tied to the introduction of solid food (11), followed by Rorγ$^+$ Tregs, coinciding with the diversification of gut microbes (*SI Appendix*, Fig. S1*A*).

To test comprehensively the homeostatic and functional relationships between these Tregs subsets, we generated a panel of conditional knockout mice with Treg-specific ablation of their defining TFs: Rorγ, Helios, Gata3, or cMaf (hereafter "TrKO"). In all these analyses, matching Cre-negative control littermates were included; as the results were essentially identical for all controls, we combined them here and in subsequent figures. Flow cytometric analysis confirmed loss of the TF (Fig. 1*C*), which was very complete, except for a small proportion of Tregs that remained Rorγ$^+$ in *Rorc* TrKO mice (because the floxed Rorc allele is somewhat refractory to Cre-mediated deletion, and/or because of only recent expression of Foxp3-cre in pTregs). These Treg-specific ablations did not lead to visible pathology in the mice, but tuned the balance between various subsets in complex ways, as illustrated in Fig. 1*D* (cell numbers), and as a compilation of Treg proportions (Fig. 1 *E* and *F*). Deficiencies in both Rorγ and cMaf led to marked decreases in Rorγ+ Tregs and corresponding increases in Helios$^+$ Tregs (Fig. 1*D*). Conversely, Helios deficiency led to an increase in Rorγ$^+$ Tregs (somewhat more modest, Fig. 1*D*) and in DN Tregs (Fig. 1*F*), the latter suggesting that some Helios+ Tregs persist in the absence of Helios, simply not recognizable as such. These results suggest that Helios+ and Rorγ+cMaf+ Tregs balance each other, likely by competing for the same homeostatic niche (or that they reciprocally inhibit each other). In contrast, the absence of Gata3 did not affect the proportions of any Treg subset (Fig. 1 *D*–*F*), suggesting that this TF does not control homeostatic regulation, rather effector functions. Unexpectedly, however, the absence of Helios led to an increase of Gata3+ Tregs (Fig. 1 *F*, *Top Left*). Thus, even though Helios and Gata3 are expressed in many of the same Tregs, Helios appears to limit Gata3 expression (unless Gata3 increases to compensate for the missing Helios).

Since colonic Tregs can emigrate to extraintestinal tissues (37, 38), we also analyzed the effect of the same mutations in extraintestinal tissues, such as the lung. In all the sites analyzed, the absence of Helios led to the same expansion of Gata3+ Tregs and DN Tregs as in the colon (Fig. 1 *F*, *Bottom* and *SI Appendix*, Fig. S1*B*). On the other hand, the reciprocal increases of Helios+ and Rorγ+ Tregs in the absence of Rorγ/cMaf or Helios, respectively, were not observed outside the colon (including in the small intestines of *Ikzf2* TrKO mice). This balancing of Helios+ by Rorγ+ Tregs may only take place in the colon because of the relative pool sizes, or because the colon is the only environment that provides the high microbial load needed to sustain Rorγ+ Tregs. In these non-colon locations, the Rorγ+ Treg pool is small and unable to significantly replace Helios+ Tregs. These results suggest that the identifying TFs of colonic Treg subsets are differently required for the differentiation of the corresponding subsets, essential for Rorγ and cMaf, less so for Helios and Gata3.

Differing Functions of Intestinal Treg Subsets. As described above, specific functions in the control of intestinal inflammation have been ascribed to intestinal Treg subsets (2), but not in a comparative manner. We first performed a broad immunophenotyping of colon immunocytes in the TrKOs (salient results displayed in Fig. 2*A*, overall data aggregated in Fig. 2*B*). Numbers of lymphocytes (T, B or ILC) were not changed by any of the mutations. Consistent with previous reports (7, 8, 17), Th1 or Th17 Tconv cells (identified by production of IFNγ and IL17) were clearly elevated in both *Rorc* and *Maf* TrKO mice, while Th2 cells (identified by Gata3 expression) were actually reduced. *Ikzf2* TrKO yielded symmetrical trends in both respects (Fig. 2*B*). These observations are consistent with overlapping functions of Rorγ+ and cMaf+ Tregs, and with our prior results (6–8, 17), but differ somewhat from other reports (6, 9), possibly due to differences in microbiota across animal facilities. *Rorc* and *Maf* TrKO mice also showed an interesting

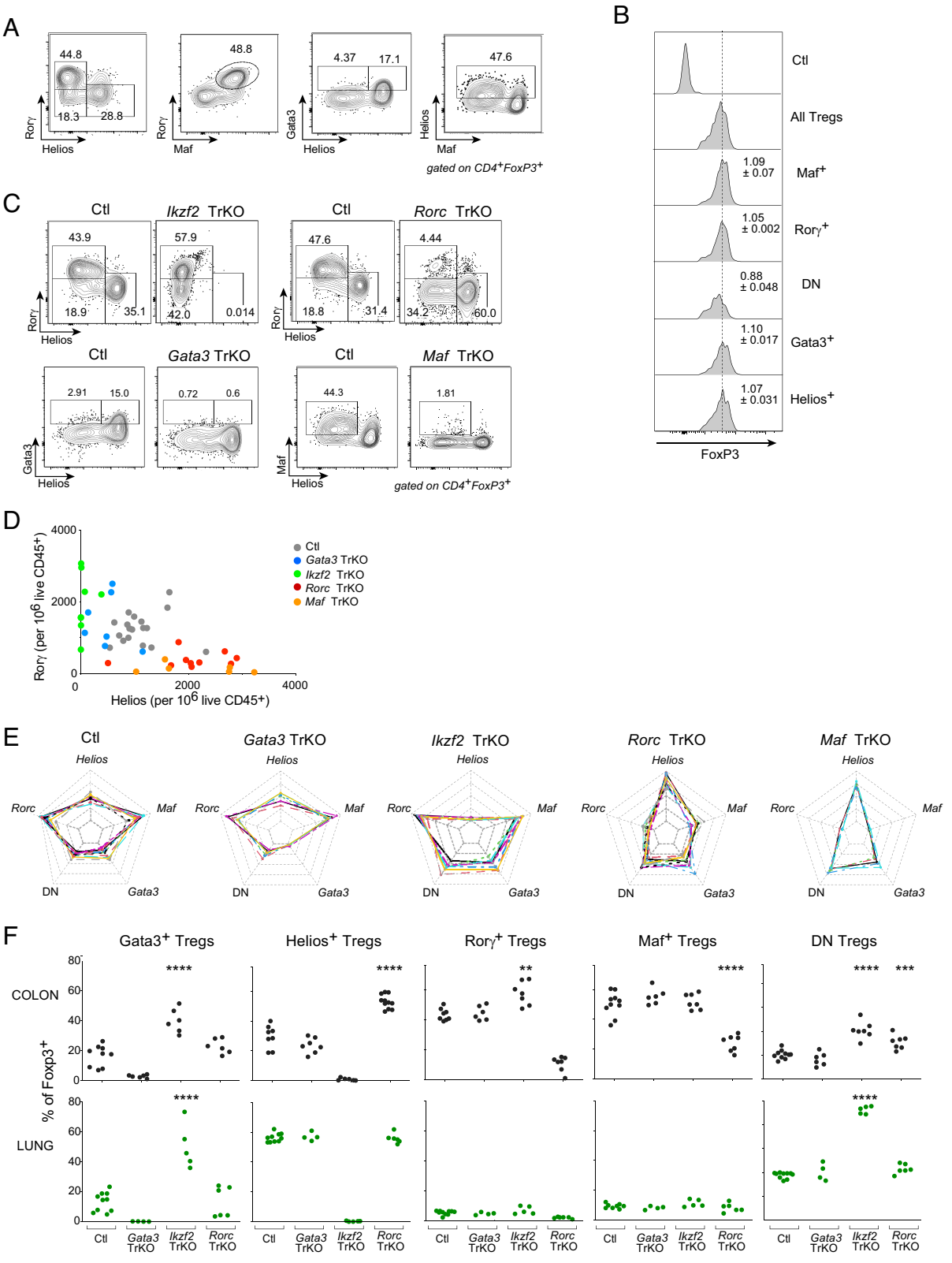

Fig. 1. Homeostatic control of colonic Treg cell subsets by key transcription factors. (*A*) Representative flow cytometry plots of Treg subset defining transcription factors gated on TCRβ+ CD4+ Foxp3+ Tregs in wild-type SPF mice on the B6 background. (*B*) Representative histograms of Mean Fluorescence Intensity (MFI) of Foxp3 expression in different Treg subsets gated as in *A*. Values represent MFI normalized to all Tregs (Foxp3+); Ctl represents all Foxp3- CD4+ T cells. (*C*) Representative flow cytometry plots of intestinal Treg subsets in each Treg-specific transcription factor knockout (TrKO) gated on TCRβ+ CD4+ Foxp3+ Tregs. (*D*) Quantification of total cell numbers of Rorγ+ Tregs vs. Helios+ Tregs gated on TCRβ+ CD4+ Foxp3+ Tregs normalized to live CD45+ cells in each TrKO and littermate controls. Littermate controls for TrKOs were pooled together for comparison and all the mice were WT for the floxed allele and Foxp3-cre+. (*E*) Radar plots of total number of Treg cells expressing key transcription factors or DN (Rorγ- Helios) in each TrKO and pooled littermate controls. Limit of the radar plot was set from 0 to 100, and colors represent individual mice. (*F*) Proportions of different Treg subsets in the colon (black) and lung (green) of each TrKO and pooled littermate controls. $^{**}P < 0.01$ and $^{****}P < 0.0001$ by the unpaired *t* test.

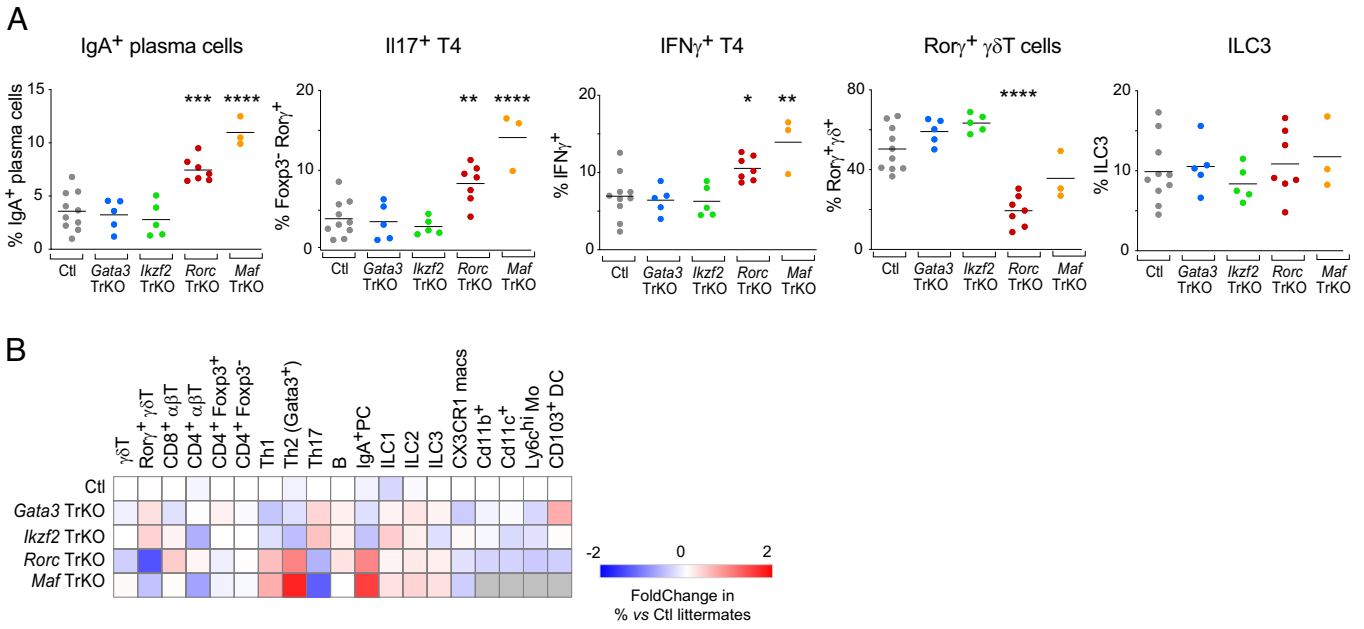

Fig. 2. Rorγ cMaf+ Tregs regulate colonic lymphocyte populations. (*A*) Quantification of selected colonic immune cell types in different TrKO and pooled littermate controls. *$P < 0.05$, **$P < 0.01$, ***$P < 0.001$, and ****$P < 0.0001$ by the unpaired *t* test. (*B*) Heatmap of relative proportions of different immune cell types (normalized to WT littermate controls) in different TrKO mice.

decrease in Rorγ-expressing γδT cells, while total γδT cells were unaffected (Fig. 2 *A* and *B*). This observation suggests a positive cooperativity between Rorγ+ Tregs and γδT cells; note that this does not extend to all Rorγ+ cells, as ILC3s, another dominant Rorγ+ cell type in the intestine, were unchanged (Fig. 2 *A* and *B*). The relationship between Rorγ$^+$ Tregs and IgA production has been unclear (6, 17, 21, 22). In line with ref. 6, we found increased IgA+ plasma cells in colons of *Rorc* and *Maf* TrKO mice, most apparent with cMaf deficiency. (Total B cell numbers were unchanged.) Thus, overall, Rorγ+cMaf+ Tregs seem to have the strongest role in regulating the numbers and activation of other immunocytes in the gut.

We then tested the various conditional knockouts in infectious or inflammatory challenge models, studying the ensuing enteric response and inflammation. For these functional studies, wt/wt cre+ littermates were used as controls, and all TrKOs were age-matched to within a week. First, we used a model of chemically induced colitis (dextran sodium sulfate—DSS—in the drinking water for 6 d + 4 d of recovery). *Rorc* TrKO mice developed more severe colitis (greater weight loss, shorter colons) compared with their littermate controls and other TrKOs (Fig. 3 *A* and *B*). DSS colitis normally entails a numeric increase in lamina propria Tregs. Here, this increase was observed with all TrKOs (Fig. 3*C*), with an increase in Rorγ+ Tregs (Fig. 3*D*), but this did not happen in *Rorc* TrKO mice, suggesting that the adaptation to colonic inflammation predominantly involves Rorγ+ Tregs. The absence of Treg expansion in *Rorc* TrKO mice under DSS may well have contributed to greater inflammation (as might their increased Th1 and Th17 cells at baseline, which persisted under DSS - *SI Appendix*, Fig. S2*A*). Interestingly, while *Gata3* TrKO mice had a normal inflammatory response to DSS (Fig. 3 *A* and *B*), particular adaptations were noted upon DSS challenge: an increase in CX3CR1+ macrophages, and a decrease in ILC2s post-DSS (*SI Appendix*, Fig. S2*B*), of unclear functional significance, but suggesting a specific role for Gata3+ Tregs in regulating the homeostasis of some immunocytes under challenge.

We also tested the response of the TrKO mouse panel during gastrointestinal infection with *Citrobacter rodentium*. We monitored bacterial colonization (cfu), weight loss, diarrhea, intestinal pathology, and analyzed various immune cell populations, including the expected Th17 response. Here, it was the *Ikzf2* TrKO mice that stood out, with an increased bacterial burden relative to control littermates and other TrKOs, and bacterial dissemination to systemic organs, here the spleen (Fig. 3 *E* and *F*). *Ikzf2* TrKO mice also had a reduced Tconv response (IL17 and IFNγ) to *C. rodentium* (Fig. 3*G*). These differences suggest a paradoxical role of Helios+ Tregs in favoring responses to this pathogen, although the effects might be due to the compensatory increase, shown above, in Rorγ+ Tregs in the absence of Helios+ Tregs (Rorγ+ Tregs acting as dominant suppressors of the *Citrobacter*-specific response).

Finally, we analyzed responses to a common protozoan parasite, *Tritrichomonas muris*, a Th2-inducing parasite (39), which is endemic in certain SPF facilities since it is not a specific pathogen that mice are routinely tested for. In order to remove the contamination, we treated the TrKO lines with metronidazole, a common treatment for *T. muris*. Because the parasite is easily transmissible, the lines became reinfected over time, but we noticed on several occasions (three times over a 12-mo period) that *Rorc* TrKO cages were most susceptible to *T. muris* reinfection, as illustrated for one time period during which reinfection was actively tracked (Fig. 3*H*). We used this opportunity to investigate the influence of Treg subsets on other immunocytes during *T. muris* infection (considering only mice with a high parasite burden). Gata3+ Tregs were consistently increased in control mice and across the different TrKOs (Fig. 3*I*; other Treg subsets being unchanged). This increase in Gata3+ Tregs in *Ikzf2* TrKOs further supported the notion that Helios is dispensable for the existence of Helios+Gata3+ Tregs. We also noted increases in ILC2s upon *T. muris* infection, as might be expected (39); this response appeared normal in *Gata3* and *Ikzf2* TrKOs but was curtailed in *Rorc* TrKOs (Fig. 3*J*). These complex results (dominant expansion of Gata3+ Tregs, ineffective antiprotozoan response in *Rorc* TrKOs) suggest an interplay between intestinal Treg subsets. They differ from previously reported results with the helminth *Heligmosomoides polygyrus*, against which responses were more effective in Rorγ+ Treg-deficient mice (9). These differing outcomes could be due to differences in the parasite (helminth

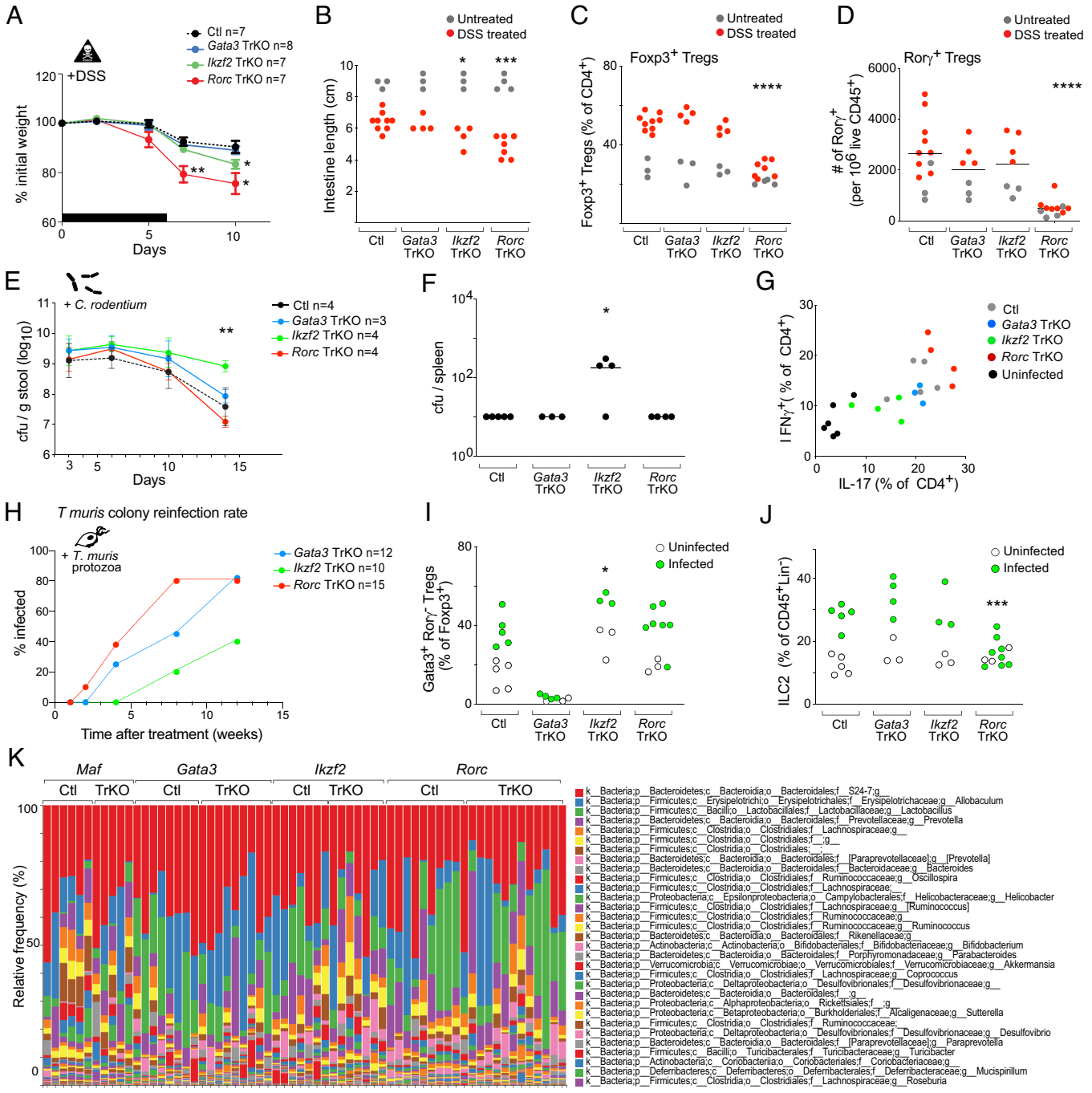

Fig. 3. Regulatory functions of colonic Treg subsets are challenge dependent. (*A*) Survival curve of different TrKO mice and controls treated with 2.5% DSS at 6 wk of age. **P* < 0.05 and ***P* < 0.01 by the unpaired *t* test. (*B*) Quantification of colon length (measured from end of cecum to rectum) post-DSS treatment in untreated (gray) and DSS-treated (red) TrKO mice and controls. **P* < 0.05 and ****P* < 0.001 by the unpaired *t* test, DSS-treated WT and knockouts. Representative picture of DSS-treated colons from TrKO mice (*Bottom*). (*C*) Proportions of Foxp3+ Tregs (gated on TCRβ+ CD4+) in untreated (gray) and DSS-treated (red) TrKO mice and controls. *****P* < 0.0001 by the unpaired *t* test, DSS-treated WT and knockouts. (*D*) Proportions of Rorγ+ Tregs (gated on TCRβ+ CD4+ Foxp3+ Helios-) in untreated (gray) and DSS-treated (red) TrKO mice and controls (*Top*). Quantification of total cell numbers of Rorγ+ Tregs normalized to live CD45+ cells in TrKO and controls. *****P* < 0.0001 by the unpaired *t* test. (*E*) *C. rodentium* cfu recovered from stool over the course of infection in TrKO mice and controls. ***P* < 0.01 by the unpaired *t* test. (*F*) *C. rodentium* cfu recovered from spleen on day 15 postinfection in TrKO mice and controls. **P* < 0.05 by the Mann–Whitney *U* test. (*G*) Representative flow cytometry plots of IFNγ vs. IL-17 in TCRβ+ CD4+ Foxp3- T cells in the colon of *C. rodentium*–infected TrKO mice and their pooled littermate controls and uninfected control mice. (*H*) Quantification of *T. muris* reinfection rate (% of mice with resurgence of *T.muris* after metronidazole treatment) in TrKO mice. (*I*) Proportions of Gata3+ Rorγ Tregs in TrKO mice highly infected with *T.muris* (see methods for low vs. high infection determination). **P* < 0.05 by the unpaired *t* test. (*J*) Proportions of Gata3+ ILC2 (% CD45+ Cd11b- Cd11c- B220- Ter119- TCRβ- TCRδ- NK1.1-) in TrKO mice highly infected with *T.muris.* ****P* < 0.001 by the unpaired *t* test. (*K*) Relative abundance of bacterial genus in stool of TrKO mice of the indicated groups generated by 16S rRNA sequencing.

vs. protozoan), or in resident microbiota (given that Ohnmacht et al noted increased Th2 in their *Rorc* TrKO mice).

As another test of differential function of intestinal Treg subsets, we assessed whether any of the TrKO lines harbored changes in their intestinal bacterial content, by performing 16S rDNA profiling of stool bacteria. Given the known issues with cage-of-origin fluctuations in microbiota, our protocol compared pairs (each TrKO had one matched control littermate; n = 6 to 12 TrKOs per line). As illustrated in Fig. 3*K* and *SI Appendix*, Fig. S3*A*, and as confirmed by the rarefaction analysis of *SI Appendix*, Fig. S3*B*, there was no

strong dysbiosis in any of the TrKO lines. We detected only a few differentially represented Amplicon Sequence Variants by QIIME2 (*SI Appendix*, Fig. S3*C*), in numbers comparable with noise estimated by permutation. Overall, these comparative analyses of host-microbe interactions indicated that the Treg subsets work in concert to maintain different aspects of intestinal immune function in the context of microbial challenges.

Genomic Identity of Intestinal Tregs. The results above indicate that these key TFs have different effects, either conditioning the existence of intestinal Treg subsets or modulating their functional capabilities. It was important, then, to determine their impact on gene expression programs, as inscribed in the genome by chromatin accessibility patterns. To systematically examine the impact of each TF on genome-wide chromatin states, we performed single-cell assay for transposase-accessible chromatin (scATAC-seq) on colon Tregs from each of the four TrKO lines and littermate controls (each in duplicate). Gene scores, chromatin-based proxies for gene expression (40), clearly delineated Helios$^+$ and Rorγ$^+$ Treg populations on a 2D UMAP (Uniform Manifold Approximation and Projection) visualization of the data (Fig. 4*A*). Relative accessibility of an ATAC-seq signature of Helios vs Rorγ Tregs from a prior study (13) supported these annotations (Fig. 4*B*). In accordance with flow cytometry results (Fig. 1*B*), *Foxp3* gene scores were similarly distributed across all Tregs (Fig. 4*A*), whereas *Gata3* predicted expression was restricted to the Helios$^+$ population and *Maf* activity spanned Rorγ$^+$, a subset of Helios$^+$, and DN populations.

We next examined the activity of TF target sites across the cell populations by computing the per-cell relative accessibility of open chromatin regions containing each TF motif (Fig. 4*C*). This mode of analysis reveals the cells in which each TF actually impacts the chromatin accessibility of its target sites (13, 42). Consistent with the gene scores, Gata3 motif accessibility was highest in the Helios$^+$ Treg population, well demarcated from Rorγ motif accessibility (Fig. 4 *C*, *Top* row). The latter was confirmed by the accessibility distribution of known Rorγ-bound sites determined by chromatin immunoprecipitation (41) (Fig. 4*D*). Helios$^+$ Tregs also had higher accessibility of NF-κB motifs, consistent with previous results identifying the activation of TNFRSF-NF-κB related

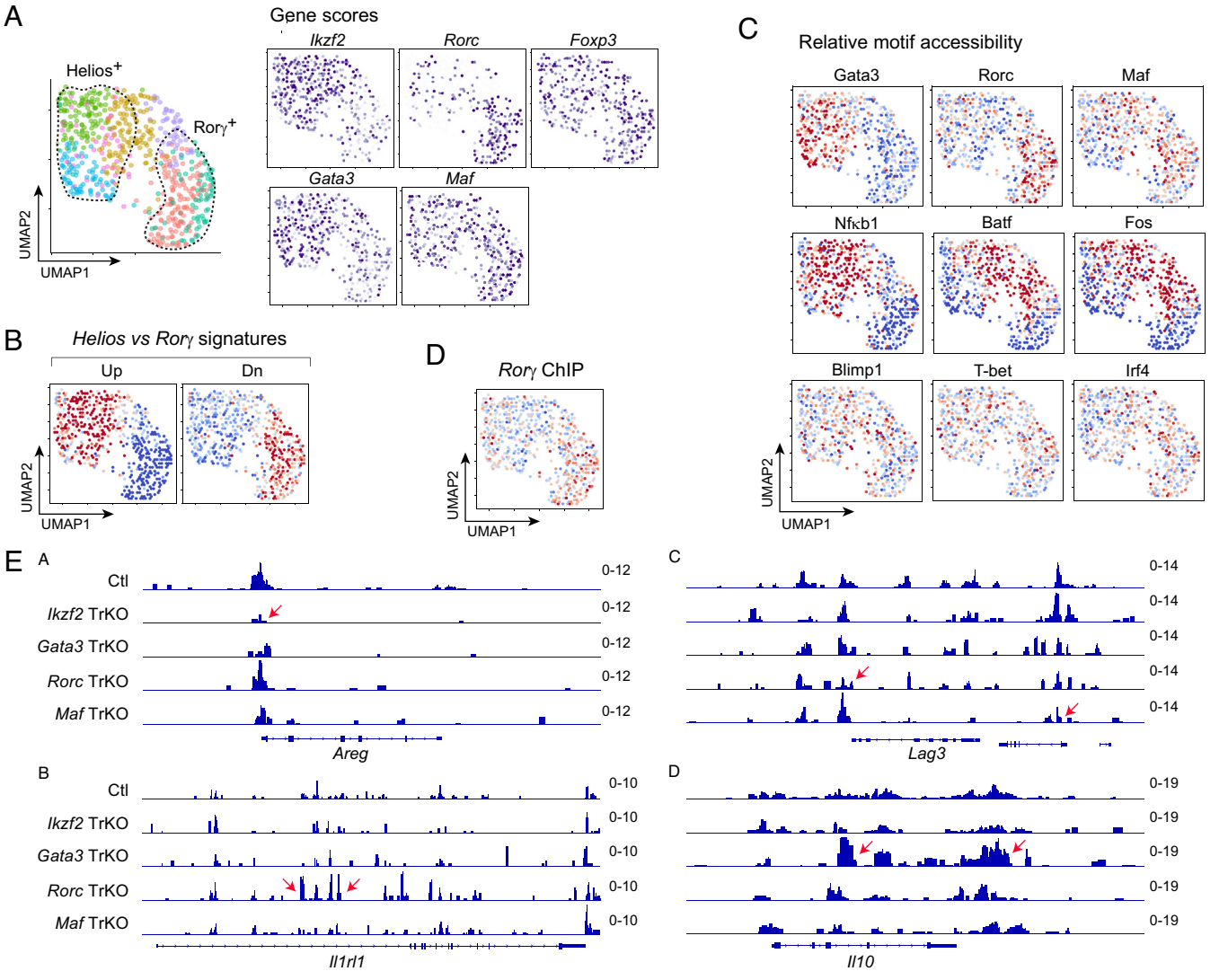

Fig. 4. Specific genomic identities within the colonic Treg space. (*A*) UMAP of scATAC-seq data, grouping cells from all mice (TrKO and WT littermates). Gene scores (chromatin-based proxy for gene expression) for select genes are overlaid onto the UMAP. (*B*) Relative per-cell accessibility (chromVAR scores) of OCRs that distinguish Helios and Rorγ populations (from ref. 13), overlaid onto UMAP from *A*. (*C*) Relative per-cell accessibility (chromVAR scores) of OCRs containing target motifs for the indicated transcription factors, overlaid onto UMAP from *A*. (*D*) Relative per-cell accessibility (chromVAR scores) of OCRs within genomic regions bound by Rorγ (from ref. 41), overlaid onto UMAP from *A*. (*E*) Aggregated accessibility profiles from the scATAC-seq data at the Areg, Il1rl1, Lag3, and Il10 loci for Tregs from Ctrl or TrKO mice. Arrows indicate regions with genotype-specific loss or gain of accessibility signal.

pathways among ST2+ Tregs (43, 44). On the other hand, other motifs also had overlapping patterns of accessibility across the Treg space, reflecting the combinatorial and interwoven nature of TF operation in Tregs (13): Maf motif-containing regions had high accessibility in most Rorγ+ Treg cells but also a segment of Helios$^+$ Tregs, in accordance with the flow cytometry data of Fig. 1; accessibility associated with BATF and AP-1 (e.g., Fos) motifs cut across Helios$^+$ and Rorγ$^+$ Tregs, through DN Tregs (Fig. 4*C*). Other TFs that have been associated with distinct functional subsets of Tregs (T-bet, IRF4, and Blimp-1 motifs) had even more diffuse activity (Fig. 4 *C*, *Bottom* row). Thus, each subpopulation of Tregs had distinct TF target activities.

Overlaying the distribution of cells from each TrKO genotype onto the UMAP space (*SI Appendix*, Fig. S4) brought a pattern consistent with the flow cytometry results of Fig. 1. Whereas WT cells were represented in Helios$^+$, Rorγ$^+$, and DN Treg populations, *Ikzf2* TrKO and *Rorc* TrKO Tregs were shifted to Rorγ$^+$ and Helios$^+$ populations respectively. Echoing the heterogenous expression and effects of cMaf, *Maf* TrKO Tregs were shifted to both the Helios+ and DN populations and away from the Rorγ$^+$ region.

Aggregated scATACseq profiles at a few example loci of relevance to Treg biology illustrate the diversity of regulatory strategies in Tregs (Fig. 4*E*). For *Areg*, a locus known to be overexpressed in Helios+ Gata3+ Tregs, the major effect was a reduction of accessibility around its promoter region in the *Ikzf2* TrKO (Fig. 4 *E*, *a*). On the other hand, around the coexpressed *Il1rl1* locus (encodes the IL33 receptor), the dominant effect was an increase in signal in the *Rorc* TrKO (Fig. 4 *E*, *b*), possibly resulting from release of Rorγ-mediated repression. (Note that this effect is not observed in the *Maf* TrKO.) For effector molecules generally associated with the Rorγ+Maf+ Treg contingent, reduced accessibility was observed at several regulatory elements within the *Lag3* gene body in *Rorc* and *Maf* TrKO Tregs (Fig. 4 *E*, *c*), suggesting a positive control by both factors. (Interestingly, the lost signal was not identical for both.) On the other hand, accessibility at regulatory regions of the *Il10* locus was strikingly boosted in *Gata3* TrKO Tregs (Fig. 4 *E*, *d*), perhaps again reflecting a derepression event. Thus, each TrKO also had consequences for the regulation of molecules important for Treg effector function, providing some molecular basis for the divergence of phenotypes following immunologic challenge, and again highlighting different regulatory strategies used by these TFs.

How Individual Microbes Mold Intestinal Tregs. Individual microbes can induce intestinal Tregs, particularly Rorγ$^+$ Tregs, in different proportions; several different mechanisms have been invoked to explain these differences (1–3). These inductive events are observed as an increase in Treg proportions; yet it is unclear what underlying cellular changes are actually involved (accelerated pTreg conversion, Treg expansion, reduced cell death, etc.) (3). It is also unknown whether the Tregs amplified by different microbes are phenotypically the same, and whether recognition of antigenic epitopes on inducing microbes is at play. To address these questions, we performed single-cell RNA sequencing (scRNAseq) on activated CD4+ T cells (TCRβ+CD4+CD44hi) from the colons of germfree mice (GF) monocolonized with individual microbes. We selected a high inducer of Rorγ+ Tregs (*Clostridium ramosum)*, an intermediate inducer (*E. coli Nissle)*, and *Peptostreptococcus magnus*, which is unable to induce Treg cells (45), also including SPF B6 mice as controls. The single-cell profiling was performed three independent times, each with biological replicates of each condition, multiplexed together with DNA "hashtags" to ensure optimal comparability (a total of 24 mice; results from one experiment are presented in the main figures, replicate in *SI Appendix*, Fig. S5*B*). Dimensionality reduction and visualization showed that all mice displayed the expected populations (based on gene signatures): naive CD4 T cells, conventional/effector T cells, and Tregs (*SI Appendix*, Fig. S5*A*). We then focused the analysis on Treg cells, which could readily be classified into three clusters, Helios$^+$, Rorγ$^+$ and DN Tregs based on previously reported signatures (46) (Fig. 5*A*). As expected, GF+ *C. ramosum* and GF+ *E. coli Nissle* had more Rorγ$^+$ Tregs compared with GF mice or GF+ *P. magnus* (Fig. 5*B*). The distribution of cells across the gene expression space suggested that the differences between Treg populations in the presence of the different microbes were mainly quantitative. Colon Tregs from mice colonized with *C. ramosum* simply had a more skewed distribution toward the Rorγ$^+$ Treg quadrant (Fig. 5*B*). Differential Gene Expression analysis, factoring out these numerically skewed distributions, uncovered no microbe-specific geneset. This conclusion was confirmed by plotting differentially expressed genes: while there were clear differences between Treg subsets, none was microbe specific (Fig. 5*C*). Thus, whatever means *C. ramosum* and *E. coli* may use to induce Rorγ, they do so by titrating more or less of the same cell, not different cell types.

We then used the dataset to generate a more refined transcriptional signature for Helios$^+$ and Rorγ$^+$ Tregs (Dataset S1 and Fig. 5 *C*–*E*). The results extended and refined our prior signatures (8, 46). Helios$^+$ Tregs were marked by increased expression of some expected genes such as *Gata3*, *Cd83*, *Il1rl1,* and *Areg*, but they also displayed an increase in NF-κB signaling-related genes, in keeping with the stronger accessibility of NF-κB motifs observed in the scATACseq data above. Rorγ$^+$ Tregs displayed increased *Maf*, *Ccr2,* and *Lag3*, but they were also marked by increased effector molecules like *Gzmb* and *Il10*, as also expected from the results above. Interestingly, the DN Treg population was characterized by stronger expression of a small geneset, including the neurotransmitter *Penk* and *Ccr8*, a molecule of interest in tumor Tregs.

To ask whether this refined signature might help sharply distinguish colonic Treg subsets, we calculated Helios+ Tregs and Rorγï€« indices for each cell and visualized the data on a 2D plot (Fig. 5*F*). Even with refined signatures, the scRNAseq profiling indicated that the demarcation between Treg subsets was not sharp, similar to what was observed between Helios$^+$, Rorγ$^+$ and DN subsets by flow cytometry. Both genomic and protein profiling suggest that while there are distinct Treg subsets, they exist in a continuum that is modulated by microbes and the local environment, rather than as discrete and distinct cell types.

TCR Selection, Diversity, and Clonality in Response to Defined Intestinal Microbes. These scRNAseq data allowed us to relate the differentiated phenotypes of Treg cells in the monocolonized mice with the composition of the TCRs expressed by each cell. The nucleotide sequences of rearranged clonotypes can serve as molecular barcodes to identified clonally related T cells, which here should help elucidate differentiation paths of the different Treg subsets. From three independent profiling experiments, we obtained the full sequence of TCRα/TCRβ pairs for 24,366 colonic CD4+ T cells from 24 GF, monocolonized (*C. ramosum* or *E. coli*), or SPF mice (with matched spleen data for 10 of these mice; Dataset S2 A and B). In line with our previous report (47), the T cell repertoire in monocolonized mice was diverse, with a broad usage of *TRAV* and *TRBV* regions (Dataset S2C).

We first analyzed these sequences for clues to the timing of differentiation of these cells, given that Treg cells generated in early periods have particular properties (48, 49), lacking N region diversity because of ontogenically delayed expression of Terminal deoxynucleotidyl Transferase (50, 51). Examination of *TRA* and *TRB* rearrangements showed that the frequency and size of N nucleotide additions, as well as base deletions from the recombining ends, were similar in colonic Helios$^+$ and Rorγ$^+$ Tregs, as well as

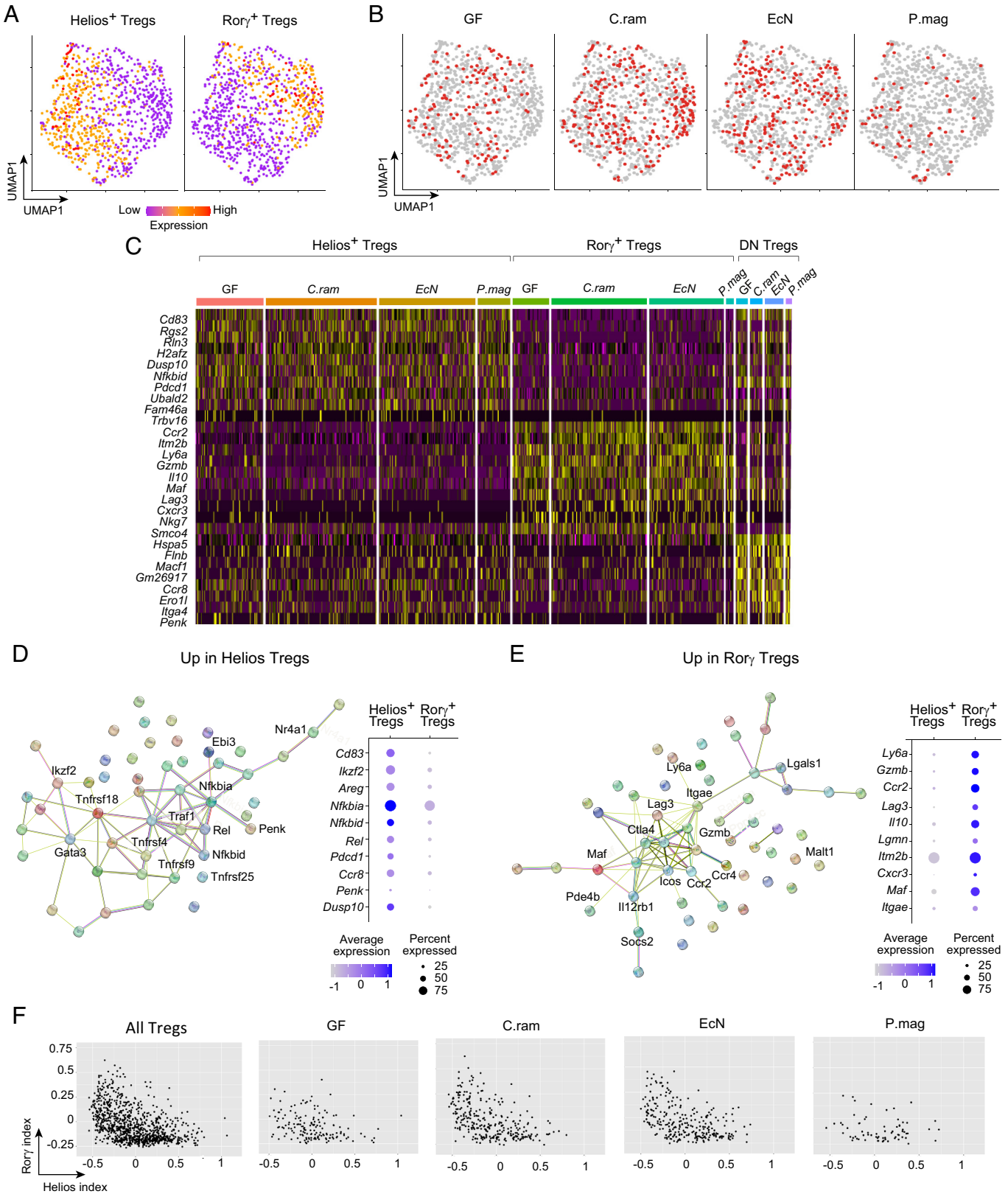

Fig. 5. Helios$^+$ Tregs and Rorγ^+ Tregs have unique transcriptional signatures that are conserved across responses to individual microbes. (*A*) UMAP projection of colonic Treg cells from a representative scRNAseq analysis of colonic Tregs in GF (germfree) and monocolonized mice, color-coded for expression of RORγ^+ and Helios$^+$ Treg gene signatures (genes in *Materials and Methods*). Repeat in *SI Appendix*, Fig. S5. (*B*) UMAP projection of colonic Treg cells as in *A*, split between hash tagged cells from different mice. Each hashtag represents an individual mouse: GF control, and GF mice monocolonized with C.ram (*C. ramosum*), EcN (*E. coli* Nissle), and P.mag (*P. magnus*). (*C*) Heatmap of top differentially expressed genes from each cluster (Helios$^+$, Rorγ^+ or DN) across the different Treg subsets from GF or monocolonized mice. (*D*) String analysis and dotplot of top differentially expressed genes in Helios$^+$ Tregs pooled from all GF and monocolonized mice. (*E*) String analysis and dotplot of top differentially expressed genes in Rorγ^+ Tregs pooled from all GF and monocolonized mice. (*F*) 2D representation of Tregs based on gene-signature scores calculated for Helios$^+$ Tregs and Rorγ^+ Tregs (genes used to calculate scores in *Materials and Methods*).

colonic Tconv, and in the same range when compared to splenic T cells from SPF mice (Dataset S2D). Furthermore, rearrangements at the *Tcra* locus are not completely uniform across ontogenic time, with a propensity for the more proximal *Va* and *Ja* genes to recombine in T cells generated in the fetal and perinatal times (52, 53). *Tcra* sequences from Rorγ$^+$ and Helios$^+$ Tregs showed a broad distribution of *TRAV* and *TRAJ* usage, comparable with that of Tconv cells in the colon, with no preference for joins involving proximal Va regions (*SI Appendix*, Fig. S6). These results suggest that neither Helios$^+$ nor Rorγ$^+$ Tregs are enriched in cells that differentiated during the fetal/perinatal period.

As previously noted, repertoires of colonic CD4+ T cells from monocolonized mice were diverse, but also included a notable proportion of clonotypes present in several cells (Fig. 6 *A* and *B*). These repeated clonotypes stemmed from clonal expansion from a common parent cell because their nucleotide sequences were completely identical at both *Tcra* and *Tcrb* loci in all cells expressing that clonotype in a given mouse, with frequent N nucleotide addition indicating that they did not derive from favored homology-driven rearrangements (*SI Appendix*, Fig. S7). In contrast, in some instances where the same protein clonotypes occurred in different mice, they were always encoded by different nucleotide sequences (*SI Appendix*, Fig. S8, showing that identical TCRα and TCRβ rearrangements in Tregs of different phenotypes did not result from favored recombination events. These expanded clonotypes were represented at similar frequencies in colonic Treg and CD44^{hi} Tconv cells, but were less frequent in Tconv cells with naïve phenotypes, indicating that they were triggered by antigen exposure. Interestingly and perhaps unexpectedly, monocolonization did not lead to narrower expansions than seen in colons of SPF mice, as evidenced by the duplication plots of Fig. 6*B*.

Clonal expansions in the colon had systemic counterparts: CD4+ T cells expressing the same clonotypes were also found in splenic CD4+ T cells from the same mouse. Overall, 4.34% of TCR clonotypes from the colon were also detected in the spleen (Dataset S2F). Conversely, TCRs in 3.28% of CD4+ T splenocytes had an analog in the colon, in monocolonized as well as SPF mice (Dataset S2G), but slightly lower in GF mice. Although we do not formally know that these shared clonotypes are of gut origin, one might speculate that gut-derived T cells are represented to the repertoire of extragut lymphoid organs at steady state.

Plotting the distribution of these expanded clonotypes showed that each was preferentially found in either Tconv or Treg cells (Fig. 6*C*). On the other hand, this preference was not complete, and many clonotypes were found in both Tconv and Treg of the same mouse (Fig. 6*C*). These occurrences did not correspond to borderline assignments of cell identity, as the cells that expressed them fell in clearly demarcated regions of the UMAP (Fig. 6*D*). One might expect to observe common TCRs between pTregs and expanded Tconv cells from which they had differentiated. Interestingly, however, annotation of Treg subsets using the signatures defined above revealed that there was essentially as much sharing between Tconv and Helios$^+$ Tregs as with Rorγ$^+$ Tregs (Dataset S2E and Fig. 6*D*). As illustrated for all the amplified clonotypes on C. *ramosum* monocolonized mice (Fig. 6*E*), there was also sharing between Helios$^+$ and Rorγ$^+$ Tregs. Our TCR sequencing results indicate that pTregs are not only Rorγ$^+$ Tregs, and/or that the phenotypes of colonic Tregs are not cast in stone, echoing the genomic observations above.

Discussion

Using a wide and complementary array of immunologic, genomic, microbiological, and functional assays, we investigated in a systematic manner the relationships between the subpopulations of colonic Treg cells that have been described in recent years and the functional involvement of the key TFs that have been associated with them. The results point to more complex interrelationships than simple dichotomies, as manifest in chromatin and transcriptional programs, the mode of operation of identifying TFs, or the homeostatic balance between subsets. Cell tracing via TCR barcodes also indicates that the oft-accepted tight relationship between Treg phenotypes and differentiative origin (tTreg==Helios$^+$ Tregs, pTreg==Rorγ$^+$ Treg) is not absolute. Instead, we propose that the setpoints resulting from microbial and other influences can modulate colonic Treg phenotypes irrespective of their locale of differentiation.

From the standpoint of the transcription factors that have been used to define these colonic Treg subpopulations, we uncovered several different modes of action. At one extreme, Gata3 seemed unnecessary to support the differentiation of any Treg subset, but influenced transcriptional activity, as manifested by chromatin accessibility profiles (the derepression of *Il10* in *Gata3* TrKO was particularly striking, Fig. 4*E*). At the other extreme, both cMaf and Rorγ seemed necessary to drive the differentiation or survival of those Tregs that express them, judging from the large swings in subset frequencies in their absence (Fig. 1)–with the caveat that it can be difficult to evaluate effects when the ablated TF is needed for subset identification. Helios seemed less required for the subset it marks, in light of the increase in DN Tregs (likely "Helios$^+$ Treg wannabes") in *Ikzf2* TrKOs, a shift that was particularly clear in the lung. Both the flow cytometry and chromatin enrichment analysis showed that factors like cMaf or Batf had broader distribution of expression and functional activity than might have been expected from prior reports.

From the standpoint of the Treg subpopulations, an important conclusion may be that they represent poles at the extreme of a spectrum, rather than cleanly demarcated entities. Several arguments bolster this view i) The gene expression profiles, where indexing colonic Tregs in the scRNAseq results according to Helios$^+$ and Rorγ$^+$ Treg signatures showed a gradation of scores, going through DN Tregs, and shifted along this crescent by the presence of specific microbes (Fig. 5*F*) ii) Helios+ and Rorγ+ Tregs (as defined by flow cytometry with TF markers) balance each other out in the TrKOs, with a reciprocal increase in the absence of one cell or the other. The implication is that they are competing for the same homeostatic niche, which is somewhat surprising since Rorγ$^+$ Tregs are strongly controlled by microbes, while Helios$^+$ Tregs are not but are strongly regulated by IL33 via ST2. Some overarching homeostatic control must be limiting the setpoint of total colonic Tregs, irrespective of their proportion, which is tuned by microbes or maternal programming iii) the blurry distinction between Helios$^+$ Tregs and Rorγ$^+$ Tregs was reinforced by the αβTCR clonotype data: several clonotypes were present in Treg cells otherwise well demarcated as Helios$^+$ or Rorγ$^+$ Tregs. This sharing demonstrates that these cells are directly related, either by sharing a common ancestor or by switching between phenotypes. Such sharing, in the context of a full polyclonal repertoire, aligns with earlier studies with constrained-diversity transgenic mice in which the same TCR clonotypes were found in both Helios$^+$ and Rorγ$^+$ Tregs (54, 55).

Consequently, the simple equation Helios$^+$ Tregs == tTregs, and Rorγ$^+$ Tregs == pTregs is no longer tenable. Cell-transfer studies with microbe-specific transgenic Tconv cells, which offer direct evidence for pTreg conversion, yielded pTregs with a predominant but not exclusive Rorγ$^+$ phenotype (7, 55, 56). Van der Veeken et al. (12) provided compelling evidence that the vast majority of pTregs are indeed Rorγ$^+$ Tregs, but this was in the context of a sharp recovery from food and microbial antigen deprivation and

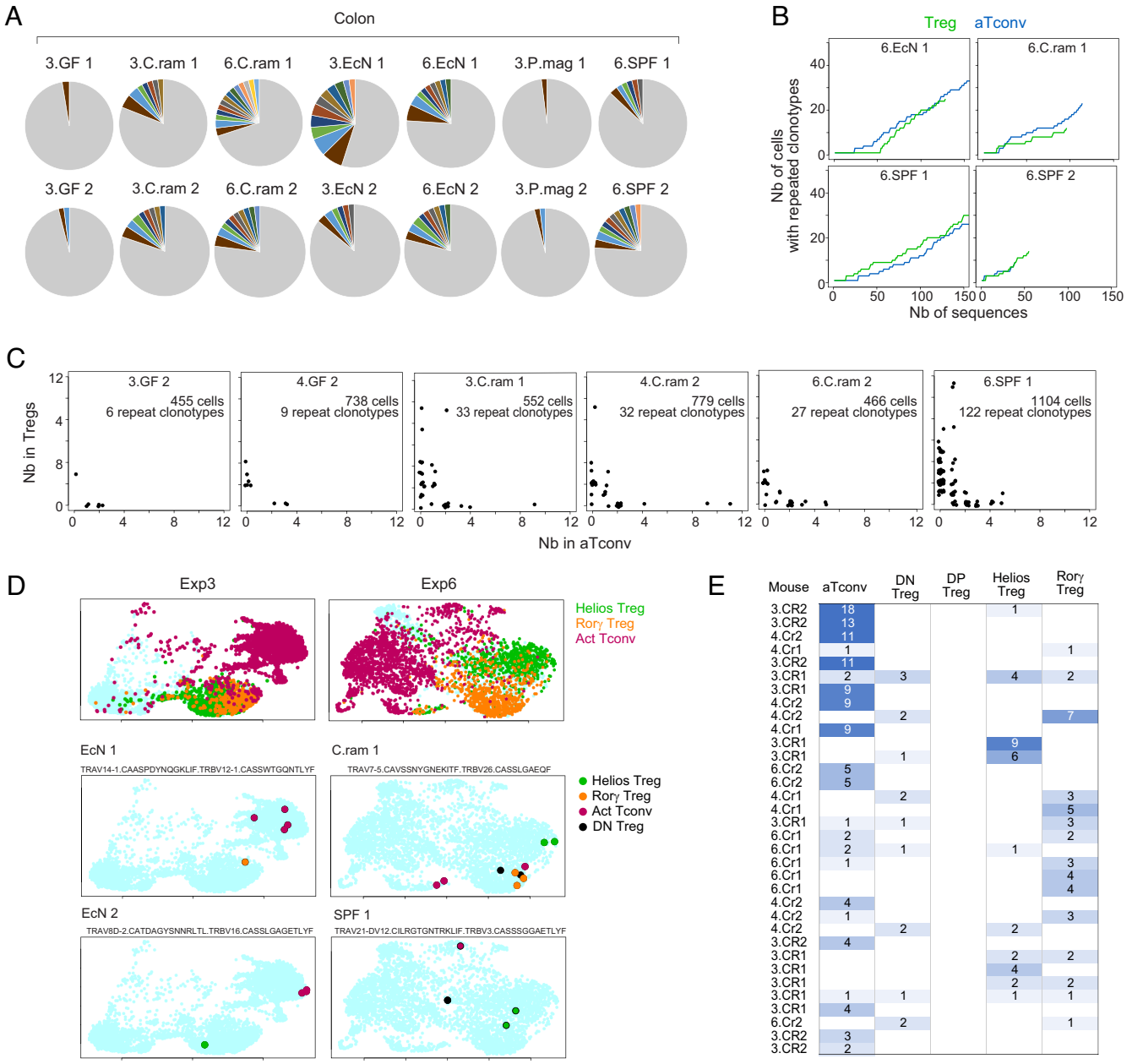

Fig. 6. TCR clonotypes between Tconv cells and various Treg subsets. (*A*) Proportion of αβ TCR clonotypes in individual mice, GF, or monocolonized colon (prefix 3, 4 and 6) and spleen (prefix 7). Nonexpanded clones in gray, colored clonotypes present in two or more cells. (*B*) Representative duplication plots (number of cells with repeated clonotypes vs cumulative number of randomly drawn sequences) in Tregs (green) and Tconv cells (blue). (*C*) Representative plots of numbers of repeated clonotypes among aTconv and Treg cells. (*D*) UMAP projection of CD4+ T cells in two separate experiments; highlights at top indicate the cell phenotype, as determined by signature gene expression; highlight on the bottom panels identify the individual cells that share the same clonotypes in the indicated mouse. (*E*) Summary table of amplified clonotypes in individual mice monocolonized by *C. ramosum* and the cell types in which they were observed.

from Treg ablation, thus in particular circumstances where pTregs are very actively generated to restore the Treg pool. In contrast, we reported earlier that the outcome of pTreg differentiation (Helios$^+$ vs. Rorγ$^+$ Treg) depended on the type of input Tconv cell (46). In addition, Rorγ can be experimentally up-regulated in tTregs (57, 58). To reconcile these observations, we propose the following model: pTreg generation, in the gut or elsewhere, is inherently agnostic as to Rorγ or Helios phenotype, and is driven by homeostatic factors that aim to regulate total Treg pool size. Rorγ or Helios phenotypes are instead controlled by independent factors, like microbial products, factors from particular APCs, maternally derived setpoints, neuronal influences, etc. that happen to dominate at the time of conversion. These factors may be particularly effective during the malleable stage of pTreg differentiation, but can also act on established tTregs. Which microbial structures or molecules coordinately swing this balance remains unclear (3).

The genomic and homeostasis results also identify an intermediate population of double-negative Tregs in the colon, not only because of their intermediate indices but also because they selectively express a particular set of genes (Fig. 5*B*). We surmise that these are equivalent to the DN population described in relation to food antigens in the small intestine (11). Do DN Tregs represent an intermediate between Helios$^+$ vs. Rorγ$^+$ Tregs or rather a stable and unrelated meta-state?

From a functional standpoint, the continuum perspective of colonic Treg cells does not detract from the specific functions associated with the different poles. In keeping with prior reports (7–9, 18), Maf+Rorγ+ Treg cells had the strongest influence on

dampening inflammation in DSS colitis, possibly because of their dominant production of Il10, which would also explain their broad effects on suppressing Teff cells of different flavors, and we confirm here the inhibition of IgA production by these Treg cells. Perhaps paradoxically, *Ikzf2* TrKO mice had a less active immune response against *C. rodentium*. We suspect that this outcome may reflect the higher proportion of Rorγ+ Tregs, rather than the dearth of Helios+ Tregs, leading to "oversuppression" of the antimicrobial response. In the same vein, the higher incidence of recurring *T. muris* infection could be interpreted as an intriguing requirement for Rorγ Tregs in the antiprotozoan response, or instead by oversuppression through the more abundant Helios+ Tregs. One should note that such interpretative uncertainty, when either a physiological effect on the primarily targeted cell or on a homeostatically connected cell type can be at play, may be a more frequent issue than realized. In terms of global influence on the gut microbiota, and in contrast to (6), none of the TrKO mice showed marked dysbiosis, defined as severe perturbations that rearrange the balance of microbial phyla and families, or as the repeated overrepresentation of a specific species or genera. Alpha-diversity was comparable in all TrKOs mice, and examination of Fig. 3*K* and *SI Appendix*, Fig. S3 shows that cage-of-origin variations are more pronounced than any mutation-specific effects. Thus, with the caveat that our experiments were only powered to identify strong dysbiosis, but not subtler effects on the microbiome network, none of the colonic Treg subpopulations seem to uniquely regulate microbial populations.

In summary, we set out to define the dynamics of colonic Treg subsets and found that while they have functional and genomic individualities, they are interconnected in many ways and that microbe and tissue-specific cues modulate their phenotypic spectrum.

Methods

Mice, Colonization, and Challenges. All mice were maintained in accordance with Harvard Medical School's Animal Care and Use Committee guidelines under IACUC protocol #IS00001257. B6 germfree and monocolonized mice and conditional knockout mice crossed to *Foxp3-cre,* were bred and maintained in our facility at Harvard Medical School under protocol IS00001257. For monocolonization, GF mice were gavaged with single bacterial species (*C. ramosum*, *P.magnus*, and *E. coli* Nissle) at 4 wk of age for 2 wk (45). For infection, 8-wk-old mice were gavaged with 1×10^9 cfu of *C. rodentium*. To check for *T. muris* colonization, PBS-suspended stool samples were assessed under the microscope. For DSS-colitis, 2.5% DSS was administered in drinking water for 6 d followed by 4 d of recovery.

Lymphocyte Analysis. Single-cell suspensions were prepared and stained (45). For scRNA-seq and T cell receptor sequencing (three independent monocolonization experiments), CD4+ T cells from distal colons of GF or monocolonized mice were sorted after hashtagging (BioLegend TotalSeq-C) and pooled for encapsulation (10× Chromium) (47). For scATAC-seq, colonic lamina propria cells were sorted for Tregs (CD4+TRCRb+CD25hi) and activated Tconvs (CD4+TRCRb+CD25loCD44hi), and hashtagged per condition using the ASAP-seq strategy (59) for low cell input samples.

Bacterial Population Profiling. Stool was collected from TrKO mice and their sex-matched control littermates, DNA was isolated from stool samples (QIAquick), and the V4 region of 16S rRNA gene amplified [515F and 806R (60)] and sequenced [Illumina MiSeq, 251 nt × 2 paired-end, data processed with QIIME2 suite (61).

Quantification and Statistical Analysis. Data are presented as mean ± SD, significance assessed by Student's *t* test or Mann–Whitney *U* test.

Data, Materials, and Software Availability. 16S microbe profiling, scRNAseq, and scATACseq are available in NCBI under accession numbers GSE241887 (62), GSE213200 (63), and GSE240657 (64).

ACKNOWLEDGMENTS. We thank Drs. X. Chi, Y. Zhu, J. Léon, and M. Wu for insightful discussions, K. Hattori, M. Sleeper, J, Nelson, L. Yang, and B. Vijaykumar for help with mice, cell sorting, and computational analysis. Supported by NIH grants AI125603 and AI150686. D.R. was supported by Damon Runyon Cancer Research Foundation (DRG 2300-17, National Mah Jongg League), K.C. by NIGMS T32GM007753 and T32GM144273 and a Harvard Stem Cell Institute MD/PhD Training Fellowship.

Author affiliations: [a]Department of Immunology, Harvard Medical School, Boston, MA 02115; and [b]Université Grenoble Alpes, Commissariat à l'Energie Atomique et aux Energies Alternatives, Centre National de la Recherche Scientifique, Interdisciplinary Research Institute of Grenoble, Laboratory of Chemistry and Biology of Metals, Grenoble 38054, France

1. J. Jacobse *et al.*, Intestinal regulatory t cells as specialized tissue-restricted immune cells in intestinal immune homeostasis and disease. *Front. Immunol.* **12**, 716499 (2021).
2. C. Cosovanu, C. Neumann, The many functions of Foxp3$^+$ regulatory T cells in the intestine *Front. Immunol.* **11**, 600973 (2020).
3. D. Ramanan *et al.*, Regulatory T cells in the face of the intestinal microbiota. *Nat. Rev. Immunol.* **23**, 749–762 (2023).
4. E. A. Wohlfert *et al.*, GATA3 controls Foxp3(+) regulatory T cell fate during inflammation in mice. *J. Clin. Invest.* **121**, 4503–4515 (2011).
5. C. Schiering *et al.*, The alarmin IL-33 promotes regulatory T-cell function in the intestine. *Nature* **513**, 564–568 (2014).
6. C. Neumann *et al.*, c-Maf-dependent Treg cell control of intestinal TH17 cells and IgA establishes host-microbiota homeostasis. *Nat. Immunol.* **20**, 471–481 (2019).
7. M. Xu *et al.*, c-MAF-dependent regulatory T cells mediate immunological tolerance to a gut pathobiont. *Nature* **554**, 373–377 (2018).
8. E. Sefik *et al.*, Individual intestinal symbionts induce a distinct population of RORg$^+$ regulatory T cells. *Science* **349**, 993–997 (2015).
9. C. Ohnmacht *et al.*, The microbiota regulates type 2 immunity through RORg$^+$ T cells. *Science* **349**, 989–993 (2015).
10. G. J. Britton *et al.*, Microbiotas from humans with inflammatory bowel disease alter the balance of gut Th17 and RORgt$^+$ regulatory T cells and exacerbate colitis in mice. *Immunity* **50**, 212–224 (2019).
11. K. S. Kim *et al.*, Dietary antigens limit mucosal immunity by inducing regulatory T cells in the small intestine. *Science* **351**, 858–863 (2016).
12. J. van der Veeken *et al.*, Genetic tracing reveals transcription factor Foxp3-dependent and Foxp3-independent functionality of peripherally induced Treg cells. *Immunity* **55**, 1173–1184 (2022).
13. K. Chowdhary *et al.*, An interwoven network of transcription factors, with divergent influences from FoxP3, underlies Treg diversity. bioRxiv [Preprint] (2023). https://doi.org/10.1101/2023.05.18.541358 (Accessed 25 May 2023).
14. A. M. Thornton *et al.*, Expression of Helios, an Ikaros transcription factor family member, differentiates thymic-derived from peripherally induced Foxp3+ T regulatory cells. *J. Immunol.* **184**, 3433–3441 (2010).
15. B. H. Yang *et al.*, Foxp3$^+$ T cells expressing RORgt represent a stable regulatory T-cell effector lineage with enhanced suppressive capacity during intestinal inflammation. *Mucosal. Immunol.* **9**, 444–457 (2016).
16. D. Zemmour *et al.*, Single-cell gene expression reveals a landscape of regulatory T cell phenotypes shaped by the TCR. *Nat. Immunol.* **19**, 291–301 (2018).
17. D. Ramanan *et al.*, An immunologic mode of multigenerational transmission governs a gut Treg setpoint. *Cell* **181**, 1276–1290 (2020).
18. J. D. Wheaton, C. H. Yeh, M. Ciofani, Cutting edge: C-Maf is required for regulatory T cells to adopt RORgt$^+$ and follicular phenotypes. *J. Immunol.* **199**, 3931–3936 (2017).
19. C. Campbell *et al.*, Extrathymically generated regulatory T cells establish a niche for intestinal border-dwelling bacteria and affect physiologic metabolite balance. *Immunity* **48**, 1245–1257 (2018).
20. A. Abdel-Gadir *et al.*, Microbiota therapy acts via a regulatory T cell MyD88/RORgt pathway to suppress food allergy. *Nat. Med.* **25**, 1164–1174 (2019).
21. Y. Cong *et al.*, A dominant, coordinated T regulatory cell-IgA response to the intestinal microbiota. *Proc. Natl. Acad. Sci. U.S.A.* **106**, 19256–19261 (2009).
22. S. Kawamoto *et al.*, Foxp3$^+$ T cells regulate immunoglobulin a selection and facilitate diversification of bacterial species responsible for immune homeostasis. *Immunity* **41**, 152–165 (2014).
23. N. R. Blatner *et al.*, Expression of RORgt marks a pathogenic regulatory T cell subset in human colon cancer. *Sci. Transl. Med.* **4**, 164ra159 (2012).
24. A. Osman *et al.*, TCF-1 controls T_{reg} cell functions that regulate inflammation, CD8$^+$ T cell cytotoxicity and severity of colon cancer. *Nat. Immunol.* **22**, 1152–1162 (2021).
25. Y. Wang, M. A. Su, Y. Y. Wan, An essential role of the transcription factor GATA-3 for the function of regulatory T cells. *Immunity* **35**, 337–348 (2011).
26. J. Yang *et al.*, Rorc restrains the potency of ST2$^+$ regulatory T cells in ameliorating intestinal graft-versus-host disease. *JCI Insight* **4**, e122014 (2019).
27. L. M. Fulton *et al.*, Attenuation of acute graft-versus-host disease in the absence of the transcription factor RORgt. *J. Immunol.* **189**, 1765–1772 (2012).
28. E. Pastille *et al.*, The IL-33/ST2 pathway shapes the regulatory T cell phenotype to promote intestinal cancer. *Mucosal. Immunol.* **12**, 990–1003 (2019).
29. M. Lyu *et al.*, ILC3s select microbiota-specific regulatory T cells to establish tolerance in the gut. *Nature* **610**, 744–751 (2022).

30. R. Kedmi *et al.*, A RORg^{+} cell instructs gut microbiota-specific Treg cell differentiation. *Nature* **610**, 737–743 (2022).
31. B. Akagbosu *et al.*, Novel antigen presenting cell imparts Treg-dependent tolerance to gut microbiota. *Nature* **610**, 752–760 (2022).
32. N. Yissachar *et al.*, An intestinal organ culture system uncovers a role for the nervous system in microbe-immune crosstalk. *Cell* **168**, 1135–1148 (2017).
33. T. Teratani *et al.*, The liver-brain-gut neural arc maintains the Treg cell niche in the gut. *Nature* **585**, 591–596 (2020).
34. Y. Yan *et al.*, Interleukin-6 produced by enteric neurons regulates the number and phenotype of microbe-responsive regulatory T cells in the gut. *Immunity.* **54**, 499–513 (2021).
35. Z. Al Nabhani *et al.*, A weaning reaction to microbiota is required for resistance to immunopathologies in the adult. *Immunity* **50**, 1276–1288 (2019).
36. K. A. Knoop *et al.*, Synchronization of mothers and offspring promotes tolerance and limits allergy. *JCI Insight* **5**, e137943 (2020).
37. A. M. Morton *et al.*, Endoscopic photoconversion reveals unexpectedly broad leukocyte trafficking to and from the gut. *Proc. Natl. Acad. Sci. U.S.A.* **111**, 6696–6701 (2014).
38. B. S. Hanna *et al.*, The gut microbiota promotes distal tissue regeneration via RORg^{+} regulatory T cell emissaries. *Immunity* **56**, 829–846 (2023).
39. M. R. Howitt *et al.*, Tuft cells, taste-chemosensory cells, orchestrate parasite type 2 immunity in the gut. *Science* **351**, 1329–1333 (2016).
40. J. M. Granja *et al.*, ArchR is a scalable software package for integrative single-cell chromatin accessibility analysis. *Nat. Genet.* **53**, 403–411 (2021).
41. H. Yoshida *et al.*, The cis-regulatory atlas of the mouse immune system. *Cell* **176**, 897–912 (2019).
42. A. N. Schep, B. Wu, J. D. Buenrostro, W. J. Greenleaf, chromVAR: Inferring transcription-factor-associated accessibility from single-cell epigenomic data. *Nat. Methods* **14**, 975–978 (2017).
43. M. Delacher *et al.*, Single-cell chromatin accessibility landscape identifies tissue repair program in human regulatory T cells. *Immunity.* **54**, 702–720 (2021).
44. R. J. Miragaia *et al.*, Single-cell transcriptomics of regulatory T cells reveals trajectories of tissue adaptation. *Immunity* **50**, 493–504 (2019).
45. N. Geva-Zatorsky *et al.*, Mining the human gut microbiota for immunomodulatory organisms. *Cell* **168**, 928–943 (2017).
46. A. Pratama, A. Schnell, D. Mathis, C. Benoist, Developmental and cellular age direct conversion of CD4^{+} T cells into RORg^{+} or Helios^{+} colon Treg cells. *J. Exp. Med* **217**, e20190428 (2020).
47. M. Sassone-Corsi *et al.*, Sequestration of gut pathobionts in intraluminal casts, a mechanism to avoid dysregulated T cell activation by pathobionts. *Proc. Natl. Acad. Sci. U.S.A.* **119**, e2209624119 (2022).
48. M. Bogue, S. Candeias, C. Benoist, D. Mathis, A special repertoire of alpha:beta T cells in neonatal mice. *EMBO J.* **10**, 3647–3654 (1991).
49. S. Yang *et al.*, Regulatory T cells generated early in life play a distinct role in maintaining self-tolerance. *Science* **348**, 589–594 (2015).
50. A. J. Feeney, Junctional sequences of fetal T cell receptor beta chains have few N regions. *J. Exp. Med.* **174**, 115–124 (1991).
51. M. Bogue, S. Gilfillan, C. Benoist, D. Mathis, Regulation of N-region diversity in antigen receptors through thymocyte differentiation and thymus ontogeny. *Proc. Natl. Acad. Sci. U.S.A.* **89**, 11011–11015 (1992).
52. N. Pasqual *et al.*, Quantitative and qualitative changes in V-J a rearrangements during mouse thymocytes differentiation: Implication for a limited T cell receptor alpha chain repertoire. *J. Exp. Med.* **196**, 1163–1173 (2002).
53. Z. Carico, M. S. Krangel, Chromatin dynamics and the development of the TCRalpha and TCRdelta repertoires. *Adv. Immunol.* **128**, 307–361 (2015).
54. E. Szurek *et al.*, Differences in expression level of helios and neuropilin-1 do not distinguish thymus-derived from extrathymically-induced CD4^{+}Foxp3^{+} regulatory T cells. *PLoS One* **10**, e0141161 (2015).
55. B. D. Solomon, C. S. Hsieh, Antigen-specific development of mucosal Foxp3^{+}RORg^{+} T cells from regulatory T cell precursors. *J. Immunol.* **197**, 3512–3519 (2016).
56. K. Nutsch *et al.*, Rapid and efficient generation of regulatory T cells to commensal antigens in the periphery. *Cell Rep.* **17**, 206–220 (2016).
57. B.-S. Kim *et al.*, Generation of RORgt^{+} antigen-specific T regulatory 17 cells from Foxp3^{+} precursors in autoimmunity. *Cell Rep.* **21**, 195–207 (2017).
58. J. Yang *et al.*, Thymus-derived Foxp3^{+} regulatory T cells upregulate RORgt expression under inflammatory conditions. *J. Mol. Med. (Berl)* **96**, 1387–1394 (2018).
59. E. P. Mimitou *et al.*, Scalable, multimodal profiling of chromatin accessibility, gene expression and protein levels in single cells. *Nat. Biotechnol.* **39**, 1246–1258 (2021).
60. J. G. Caporaso *et al.*, QIIME allows analysis of high-throughput community sequencing data. *Nat. Methods* **7**, 335–336 (2010).
61. E. Bolyen *et al.*, Reproducible, interactive, scalable and extensible microbiome data science using QIIME 2. *Nat. Biotechnol.* **37**, 852–857 (2019).
62. D. Ramanan, D. Mathis, C. Benoist, Composition of colonic microbes in mice deficient in intestinal Treg subsets. Gene Expression Omnibus. https://www.ncbi.nlm.nih.gov/geo/query/acc.cgi?acc=GSE241887. Deposited 30 August 2023.
63. M. Sassone-Corsi, D. Ramanan, D. Mathis, C. Benoist, Impact of bacterial mono-colonization on intestinal and splenic CD4 T cells responses. Gene Expression Omnibus. https://www.ncbi.nlm.nih.gov/geo/query/acc.cgi?acc=GSE213200. Deposited 12 September 2022.
64. D. Ramanan, K. Chowdhary, C. Benoist, Homeostatic, repertoire and transcriptional relationships between colon T regulatory cell subsets. Gene Expression Omnibus. https://www.ncbi.nlm.nih.gov/geo/query/acc.cgi?acc=GSE240657. Deposited 11 August 2023.